Topological and geometrical entanglement in a model of circular DNA undergoing denaturation

M. Baiesi[1,a], E. Orlandini[1], and A.L. Stella[1,2]

[1] INFM-Dipartimento di Fisica, Università di Padova, 35131 Padova, Italy
[2] Sezione INFN, Università di Padova, 35131 Padova, Italy

Abstract. The linking number (topological entanglement) and the writhe (geometrical entanglement) of a model of circular double stranded DNA undergoing a thermal denaturation transition are investigated by Monte Carlo simulations. By allowing the linking number to fluctuate freely in equilibrium we see that the linking probability undergoes an abrupt variation (first-order) at the denaturation transition, and stays close to 1 in the whole native phase. The average linking number is almost zero in the denatured phase and grows as the square root of the chain length, N, in the native phase. The writhe of the two strands grows as $\sqrt{N}$ in both phases.

1 Introduction

It is well known that topological (knotting and linking) and geometrical (supercoiling) entanglements in long DNA molecules are critical to the functioning of the cell [1]. For this reason there exist enzymes such as topoisomerases and recombinases which facilitate cellular metabolism by changing the geometry and the topology of DNA [2–5].

For closed loops of double-stranded DNA (dsDNA) the consequences of the double-helix linking number Lk being non zero have been extensively studied [6–9]. For example, it is known that a large imposed linking number leads the chain to twist upon itself. This is the phenomenon of *supercoiling* in DNA, analogous to the familiar buckling of a twisted tube or wire [10]. The linking entanglement is believed to play an important role in structural transitions of double stranded chains such as local denaturation and cruciform structures formation. In particular at the melting transition it is possible that progressive supercoiling of the native part of the molecule affects the denaturation process and there are indeed experimental indications that supercoiled structures denature at higher temperature and over a broader temperature range than DNA molecules in the relaxed state [11,12]. However, despite this evidence of the effects that topology and geometry can have on the denaturation transitions of circular

dsDNA's, theoretical studies of thermal denaturation have in general neglected this aspect up to know. Indeed, starting with the seminal work of Poland and Sheraga [13], statistical mechanics studies of denaturation have focussed mainly on the nature of the transition and on how this depends on properties such as the self and mutual avoidance of the strands [14–16], the bending rigidity of the bound segments [17], or the inhomogeneity of the base pair sequence [18]. An attempt to include topological constraints in statistical models of thermal denaturation has been made recently by Rudnick and Bruinsma [19]. This study, carried on within the Poland and Sheraga model, is based on the introduction at mean field level of an elastic strain energy concentrated in the native part of the chain. Their model completely neglects the $3D$ nature of the entanglement complexity of the double stranded chain. In order to reach more firm conclusions about the effects of the torsional strain on the nature of thermal denaturation, one needs of course models in which these effects coexist with a realistic representation of the geometrical and topological entanglement of DNA.

In the present article we address the problem of describing properly the topological and geometrical complexity of DNA when it undergoes the denaturation transition. More precisely, we set up a model in which, while denaturation is induced by energetic factors not directly related to the entanglement complexity of the chain, the topological and geometrical properties can be

[a] e-mail: baiesi@pd.infn.it

meaningfully represented and monitored in equilibrium. This approach, which has some complementarity with respect to that of reference [19], should be seen as a first step towards descriptions that embody also torsional strain interactions induced by a linking constraint, which are not considered here.

2 Model and phase diagram

We consider a model of circular double stranded DNA where the two strands are mimicked by two non-overlapping self-avoiding polygons (SAP) of N edges on the cubic lattice. Suitable short range attractive interactions between homologous pairs of monomers of the two strands are then considered to induce the formation of the double structure. Each SAP is rooted at one vertex and the rooted vertices of the two SAP's are fixed to remain always a lattice distance apart. We identify the configuration ω of the two SAP's by the positions $\mathbf{r_1}(\mathbf{i})$ and $\mathbf{r_2}(\mathbf{i})$, $i = 1, 2, \ldots N$, of the visited lattice vertices. A binding energy $-\epsilon$, $(\epsilon > 0)$ is associated to each pair of vertices $(\mathbf{r_1}(\mathbf{i}), \mathbf{r_2}(\mathbf{j}))$ having $i = j$ and distance $|\mathbf{r_1}(\mathbf{i}) - \mathbf{r_2}(\mathbf{j})| \leq \sqrt{3}$ in lattice units. We call such kind of pair a *contact*. The extension of the range of the interaction to the third neighbors is suggested by the need of conferring a reasonable degree of flexibility to the two SAP's when they are bound together to form the double chain structure. At low temperature, shorter ranges of interaction would indeed cause double stranded (ribbon-like) structures that are quite rigid [20] and, even if rigidity effects are not expected to be relevant for the asymptotic features of the denaturation transition [16], their reduction can avoid slow crossover effects.

The Hamiltonian of a dsDNA configuration ω is

$$H(\omega) \equiv -m(\omega), \qquad (1)$$

where $m(\omega)$ is the number of contacts as defined above. The canonical partition function Z at an inverse temperature $\beta = 1/T$ is

$$Z \equiv \sum_{\omega} e^{-\beta H(\omega)} \qquad (2)$$

and most thermodynamic quantities follow as weighted averages normalized by Z. The binding energy is taken to be the same all along the strand, *i.e.*, we neglect the heterogeneity of base pair interactions of specific sequences. This is a reasonable first approximation if we consider that a single unit lattice step should correspond to a persistence length of the strands. So ϵ represents in fact an average binding energy for a set of several base pairs. At $\beta = 0$ the two strands behave as independent SAP's, whereas at sufficiently high values of β the two SAP's are bound, *i.e* a macroscopic number ($\propto N$) of contacts occurs. In analogy with similar previously studied models [14,20], a melting transition is expected to occur at some $\beta = \beta_c$. Coming from low temperatures, this transition is driven by the formation of denatured loops, whose length can be measured
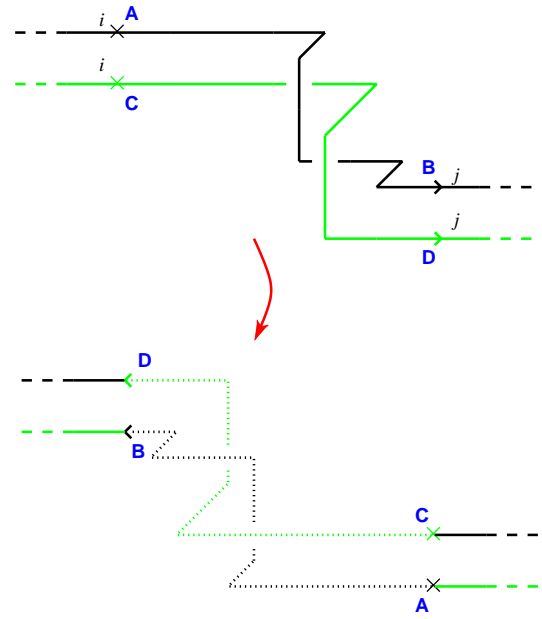

Fig. 1. Schematic representation of the double-inversion move: two monomers i and j are selected randomly (with $i < j$) along the SAP sequence and a move is tried if the positions $\mathbf{r_1}(\mathbf{i})$ and $\mathbf{r_1}(\mathbf{j})$ (first SAP) and $\mathbf{r_2}(\mathbf{i})$ and $\mathbf{r_2}(\mathbf{j})$ (second SAP) satisfy the relation $\mathbf{r_1}(\mathbf{i}) - \mathbf{r_2}(\mathbf{i}) = \mathbf{r_1}(\mathbf{j}) - \mathbf{r_2}(\mathbf{j})$. The proposed move is an inversion of the portion of the two chains between i and j with respect to their middle point $\mathbf{r_m} = 1/2(\mathbf{r_1}(\mathbf{i}) + \mathbf{r_2}(\mathbf{j}))$.

by the number of unbound monomers ℓ comprised between two consecutive contacts of the corresponding strand segments [15,16].

Configurations have been sampled by Monte Carlo (MC) methods. Since the system is strongly interacting we have adopted a multiple Markov chain approach in which one samples simultaneously at a variety of different temperatures and "swaps" configurations between contiguous temperatures. The swap probability is chosen so that the limit distribution of the process is the product of the Boltzmann distributions at the individual temperatures [21]. The underlying (symmetric) Markov chain used is based on a combination of pivot moves for SAP [22] and of local moves [23]. In addition, to increase the mobility of the MC sampling in the native phase, we have introduced a new, "double inversion" move (see Fig. 1). This move has the advantage that it may change the mutual entanglement of two SAP's while keeping the number of contacts fixed; it is thus particularly effective in sampling configurations in which the two strands are strongly bound and linked. The result of applying this move is a net increase of the mobility of the MC in the low temperature, native phase.

In our simulations, each MC step consists of $O(1)$ pivot and double inversion moves and $O(N)$ local moves. By running in parallel a number $M \approx 30$ of Markov chains we are able to obtain good sampling for chains up to $2N = 1200$, from $\beta = 0$ up to $\beta = 1.1$. For all lengths we obtain samples with at least 10^5 independent data points
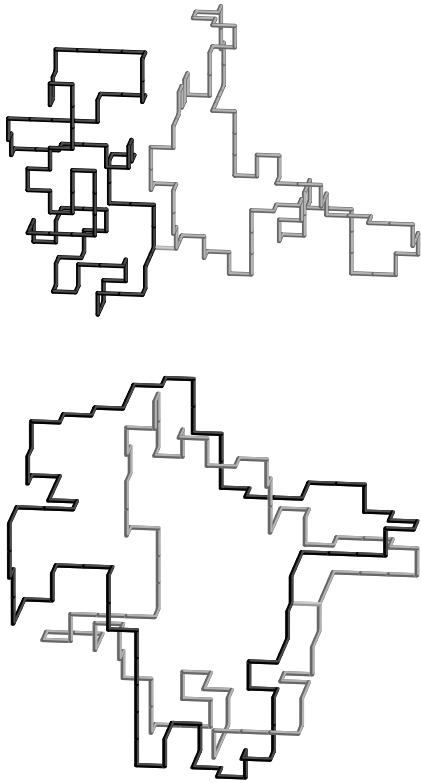
Fig. 2. Snapshots of typical configurations at β lower (top) and higher (bottom) than the denaturation inverse temperature β_c.

Fig. 3. Plot of the energy density $\langle H \rangle / N$ as a function of β, for $N = 100(\circ)$, $150(\times)$, $200(\triangle)$, $300(\square)$, $400(\triangledown)$, $500(\diamond)$, $600(\bullet)$. As N increases, two behaviors are clearly distinguished: for $\beta \lesssim 0.9$, $\langle H \rangle / N \to 0$, while $\langle H \rangle / N \to$const. for $\beta \gtrsim 0.9$.

Fig. 4. Plot of the specific heat C as a function of β, for the same values of N as in Figure 3. Note that each curve displays a maximum that increases as N increases. Since we expect the transition to be asymptotically first-order ($\phi = 1, c > 2$), the peaks should develop into a δ-like singularity as $N \to \infty$.

for almost all β's considered. Only for the highest β's the correlation of successive samples reduces the number of independent data points to $\sim 10^4$. To interpolate the obtained data at intermediate temperatures we have used the multiple histogram method [24].

In order to study the entanglement of the configurations as a function of temperature and in particular at the melting transition, we need first to characterize the phase diagram of the model and to estimate β_c. Two regimes are manifestly present: a low β regime characterized by two unbound and independent SAP's, and a high β phase dominated by configurations in which the two strands are strongly bound (see Fig. 2).

A transition between these two regimes is suggested by the behavior of the average energy per monomer

$$\frac{\langle H \rangle}{N} = \frac{1}{ZN} \sum_{\omega} H(w) \mathrm{e}^{-\beta H(\omega)} \qquad (3)$$

as a function of β (see Fig. 3).

Indeed from Figure 3 we note that, for $\beta < \beta_c \approx 0.9$, $\langle H \rangle / N$ goes to zero as $N \to \infty$ whereas $\langle H \rangle / N$ reaches a finite limit for $\beta > \beta_c$. The crossover between these regimes is particularly sharp and this is confirmed by the behavior of the specific heat

$$C(N, \beta) \equiv -\frac{\beta^2}{N} \frac{\partial \langle H \rangle}{\partial \beta} = \frac{\beta^2}{N} (\langle H^2 \rangle - \langle H \rangle^2) \qquad (4)$$
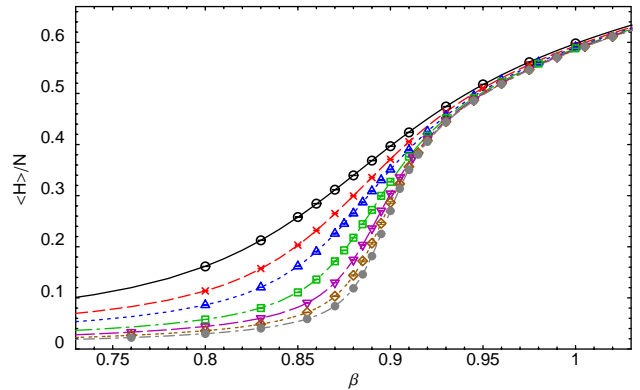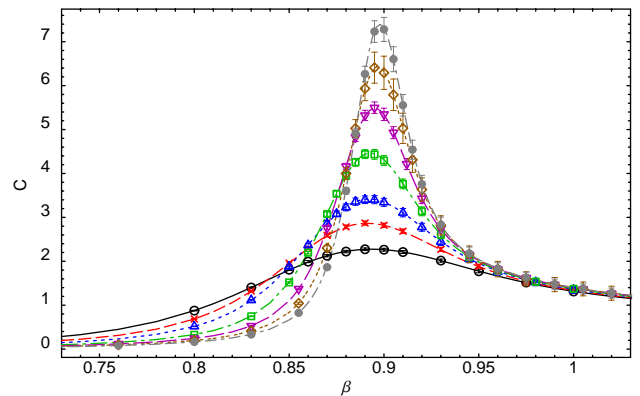
as a function of β, which is plotted in Figure 4. In the proximity of β_c the singular part of the specific heat is expected to scale as

$$C \simeq N^{2\phi-1} f((\beta - \beta_c) N^\phi), \qquad (5)$$

where f is a scaling function and ϕ is the crossover exponent. Since for large N one has $C_{\max}(N, \beta_c(N)) = \max_\beta C(N, \beta) \sim N^{2\phi-1}$, by a linear fit of $\ln C_{\max}$ *vs.* $\ln N$ we obtain $\phi = 0.9(1)$. From equation (5) we expect also $(\beta - \beta_c) \sim N^{-\phi}$ and by extrapolating $\beta_c(N)$ *vs.* $1/N^\phi$, with ϕ given by the previous estimate, we obtain $\beta_c = 0.905(5)$.

As in other recently studied models of DNA denaturation [15,16], it is useful to look at the probability distribution $P(\ell, N)$ of the denatured loops of length ℓ. Indeed, it turns out that for $\beta < \beta_c$ $P(\ell, N) \sim \ell^{-c} f(l/N)$ with an exponent c connected to ϕ by the relation $\phi = \min\{c-1, 1\}$, if $c > 1$. Hence, a continuous transition corresponds to
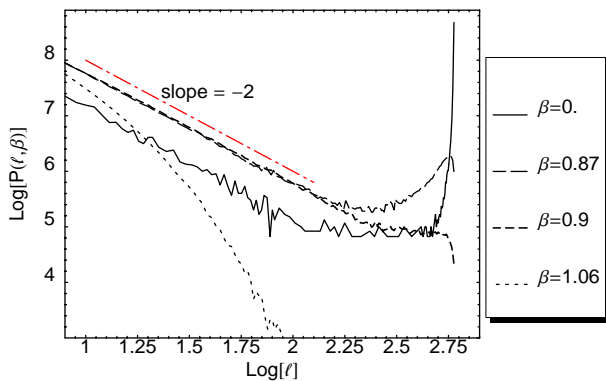
Fig. 5. A log-log plot of the loop probability distribution $P(\ell, N = 600)$, for different β values. For $\beta \leq 0.9$ the curves display a power law behavior, while for $\beta = 1.06$ strong cut-off effects are present.

$c < 2$, while $c > 2$ gives $\phi = 1$ and a first order denaturation. To estimate c, we examine the $P(\ell, N = 600)$, shown in Figure 5, for different β's. Its slope at $\beta = 0.9$ and in the range $10 \leq \ell \leq 180$ has the borderline value $c = 2.01(5)$. This value is slightly lower than the one predicted for somewhat simpler models considered recently, in which the geometry of contacts is drastically simplified to the extent that linking entanglement cannot be defined for the two strands [16]. This small discrepancy is most probably due to the relatively shorter chains considered here and to the less accurate determination of β_c. We believe that the transition has a first order character. This conclusion is also supported by the behavior of the linking probability discussed below. It should also be taken into account that the present model has interactions which induce some bending rigidity of the double stranded structure. These effects have already been shown in [16] to produce a slight lowering of the effective c for finite N.

3 Mutual entanglement: linking number

The topological and geometrical properties of the model are then studied by looking at the behavior, as a function of T, respectively of the linking probability and of the writhe, which gives a measure of the degree of supercoiling [25].

In this section we ask for the probability that the two strands are linked as a function of T and, in particular, its behavior at the melting transition, whose location has been estimated in the previous section. First let us be clear on what we mean by two linked curves.

Two disjoint simple closed curves $\mathcal{C}_1$ and $\mathcal{C}_2$ are *topologically unlinked* if there is a homeomorphism of R^3 onto itself, $H: R^3 \to R^3$, such that the images $H(\mathcal{C}_1)$ and $H(\mathcal{C}_2)$ can be separated by a plane [26].

Another notion of linking is given by the *homological linking* definition. $\mathcal{C}_1$ is *homologically unlinked* from $\mathcal{C}_2$ if
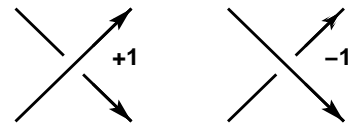

Fig. 6. Positive and negative crossings determined a by left-hand rule.

$\mathcal{C}_1$ bounds an orientable surface which is disjoint from $\mathcal{C}_2$. Homological linking is a symmetric relation, and homological linking implies topological linking. In this paper we shall be concerned just with homological linking. The reasons to restrict ourselves to this definition of linking are twofold. In first place this is the simplest topological property to be checked computationally. In addition, despite the fact that homological linking is the weakest detector of links, it is known to be a good indicator of topological linking for configurations in which the two SAP's are strongly interpenetrating [27]. This is the situation that we expect to occur in the proximity of the denaturation transition.

A method to detect whether or not the two strands are homologically linked consists in orienting each of the two strands $\mathcal{C}_1$ and $\mathcal{C}_2$, and to project them onto a plane. In general the projection will have crossings and, for almost all projection directions, these will be transverse so that we can assign a value $+1$ or -1, according to the orientation of the crossing (see Fig. 6). The sum of these crossing numbers is called the *linking number* of the two curves, $Lk(\mathcal{C}_1, \mathcal{C}_2)$, and the two curves are homologically linked if and only if $Lk(\mathcal{C}_1, \mathcal{C}_2) \neq 0$ [26].

In Figure 7 we show the probability, P_{hom}, for the two circular strands to be homologically linked (*i.e.* having non-zero linking number) as a function of β and for different N values. The qualitative trends are clear. The linking probability increases with increasing β at fixed N. In particular at high β, (*i.e.* in the native phase), the linking probability is very close to 1, indicating that the double stranded structures are very likely to be linked *even for finite values of N*. It is interesting to notice that, in the proximity of the denaturation transition, the change in slope is very sharp, suggesting a possible discontinuity in the value of P_{hom}. This possible feature is more evident in Figure 8 where P_{hom} has been plotted as a function of $1/N$ for different β values. It seems clear that for $\beta < \beta_c$ *i.e.* above the denaturation transition, the curves extrapolate (as $N \to \infty$) to values $\bar{p} = \bar{p}(\beta)$ with $\bar{p}$ varying gradually, but sensibly, with β, whereas as soon as $\beta > \beta_c$ (*i.e.* in the bounded region) the limiting linking probability is very close to 1. At $\beta = 0$ the linking probability seems to extrapolate to a value $\bar{p}(0) \approx 0.2$. A more detailed analysis of the linking probability can be carried out by looking at the probability, $P_{Lk}(\beta)$, to have a given linking number Lk. In Figure 9, $P_{Lk}(\beta)$ has been plotted as a function of β for different Lk values and for $N = 400$. Again one can observe that at $\beta \simeq \beta_c$ there is an abrupt decay of $P_0(\beta)$ (*i.e.* the probability to be unlinked) to which corresponds
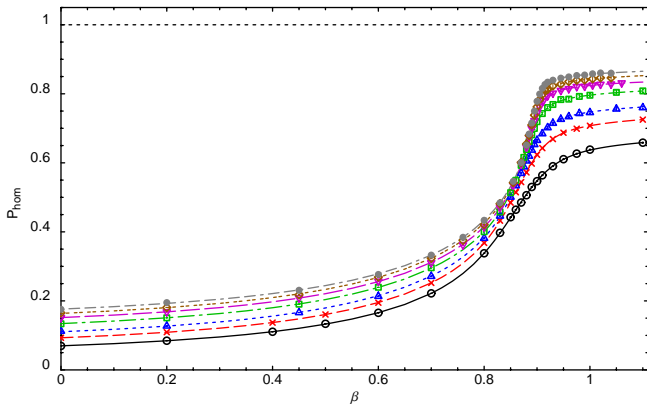
Fig. 7. Plot of the linking probability as a function of β. Different curves correspond to different N values, as in Figure 3. In correspondence to the transition ($\beta \approx 0.9$) an abrupt jump of P_{hom} develops.
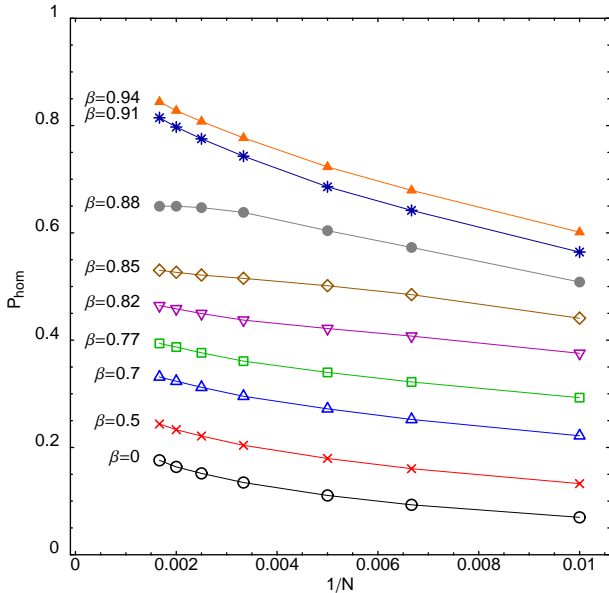

Fig. 9. Plot of the probability of having a fixed linking number $Lk \geq 0$ as a function of β for $N = 400$. In the plot we have just considered positive values of Lk since $P_{-Lk}(\beta) = P_{Lk}(\beta)$.

Fig. 8. Plot of P_{hom} as a function of $1/N$ for different β values. By observing that $\beta = 0.88$ is below the transition point $\beta_c = 0.905(5)$, while $\beta = 0.91$ is just above β_c, it is evident that a change in the asymptotic behavior of the curves takes place in proximity of the transition.

ergy are associated here to the twist of the bounded DNA segments.

In Figure 10 we show the average of the absolute value of the linking number $\langle |Lk| \rangle$ as a function of β for various values of N. In the whole range of $\beta < \beta_c$ and for each N, $\langle |Lk| \rangle$ is very close to zero and grows very slowly with N. As $\beta \geq \beta_c$ there is an abrupt change to a regime characterized by a more rapid increase of $\langle |Lk| \rangle$ as a function of N. By assuming that for $\beta > \beta_c$ the following power law behavior holds

$$\langle |Lk| \rangle \sim N^{\sigma} \tag{6}$$

we can estimate the σ exponent through a simple linear fit of $\log \langle |Lk| \rangle$ *vs.* $\log N$. This gives

$$\sigma = 0.52 \pm 0.01 \tag{7}$$

for the whole range $\beta > \beta_c$ (see Fig. 11). It is interesting to notice that such estimate is in good agreement with the one obtained for the two boundary curves of an orientable lattice ribbon model [28]. In other words the low temperature phase of our model presents the same asymptotic topological properties as those of a lattice ribbon model introduced some time ago to describe the entanglement complexity of double-stranded molecules in a good solvent [29,30]. This is what one should expect for a model of dsDNA in the native state and confirms the adequacy of our model.

A further indication of the scaling behavior in equation (6) is shown in the inset of Figure 10 where we plot $\langle |Lk| \rangle / \sqrt{N}$ *vs.* β: clearly in the range $\beta > \beta_c$ all the data collapse onto a single curve whereas in the denatured phase (*i.e.* $\beta < \beta_c$) the curve approaches zero as N increases.

Notice from Figure 10 that even in the native phase $\langle |Lk| \rangle$ is not very big: for example, $\langle |Lk| \rangle \approx 2.5$ for $N = 600$. However the distribution of the linking number turns

a sharp increase in all the probabilities of having nonzero values of Lk. For $\beta \gg \beta_c$ it seems that $P_0(\beta)$ goes to a constant different from zero; this is however a finite size effect (the plot is for $N = 400$) and as N increases $P_0(\beta)$ decreases monotonically.

The evidence of a discontinuity of P_{hom} presented above supports the first order character of the denaturation transition of the model. This should be expected in view of the results of references [15,16] and of the fact that Lk is unrestricted and no contributions to the en-
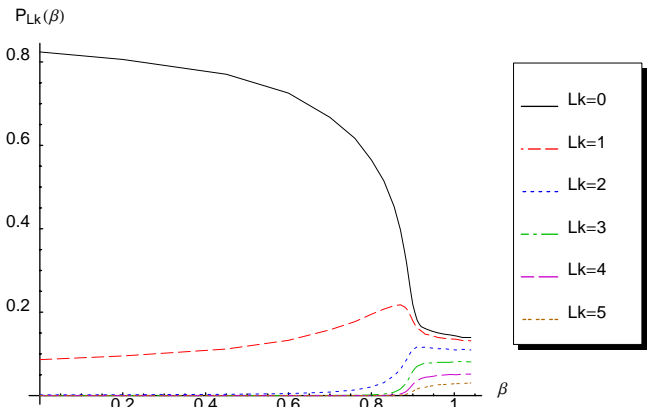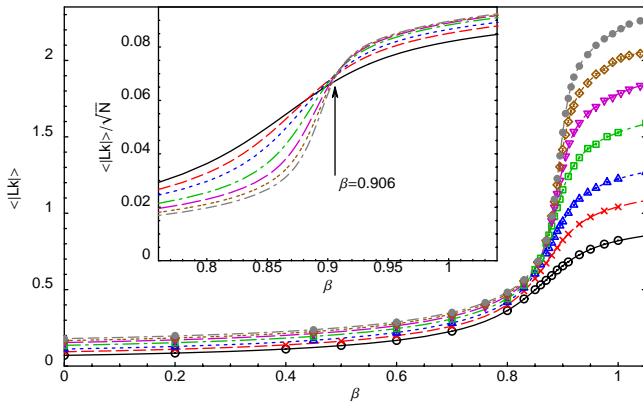
Fig. 10. Average of the absolute value of Lk as a function of β. Different curves correspond to different N values, as in Figure 3. Notice that for $\beta \geq \beta_c$ there is an abrupt increase of the average linking number. The scaling of $\langle|Lk|\rangle$ is consistent with the form $\langle|Lk|\rangle \sim \sqrt{N}$ and with $\beta_c = 0.905(5)$, as shown in the inset.

Fig. 11. Effective exponent σ of the linking number ($\triangle$) and ζ of the writhe ($\triangleright$) as a function of β. The variations of ζ close to the transition are probably due to corrections to the scaling equation (8) that are much larger than the statistical errors displayed in the figure.

out to be quite spread in the low temperature regime and configurations having relatively high values of Lk have been found. For instance, for $N = 600$ configurations with Lk up to 14 have been sampled.

4 Geometrical entanglement: writhe

In this section we analyze the geometrical entanglement of the system as a function of temperature by computing the writhe of each SAP separately. In order to define a writhe, consider any simple closed curve in R^3, and project it onto R^2 in some chosen direction. In general the projection will have crossings and, for almost all projection directions, these crossings will be transverse, so that we can associate a sign $+1$ or -1 with each crossing. For this projection we perform the sum of these signed crossing numbers and average over all possible projection directions. This average quantity is the writhe Wr of the curve [7]. The writhe is a geometrical quantity (since it is not invariant under ambient isotopy) and, contrary to the integer Lk, it is a real number measuring the extent to which the strand is supercoiled. In principle one needs to average the sum of the signed crossing numbers over all (regular) projections but there is a useful theorem [31] which considerably simplifies the calculation for polygons on the simple cubic lattice. Indeed for a SAP in the cubic lattice, the computation of the writhe equals the average of the linking numbers of the given SAP and its push-offs (translate through a sufficiently small distance) into four non-antipodal octants [31].

For a single non-interacting SAP it is known that the mean of the absolute value of the writhe behaves as [32]

$$\langle|Wr|\rangle \sim N^\zeta, \tag{8}$$

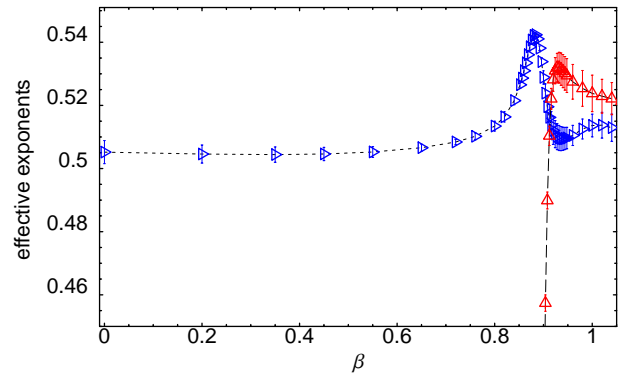and we expect the same power law behavior for our model in the denatured regime (i.e. $\beta < \beta_c$) where the two

strands behave essentially as two independent SAP's. As a check we estimate the ζ exponent at $\beta = 0$ assuming the scaling behavior (8). By a linear fit of the log-log plot of the N dependence of $\langle|Wr|\rangle$ at $\beta = 0$, and with $N \in \{300, 400, 500, 600\}$, we obtain

$$\zeta = 0.505(4), \tag{9}$$

in full agreement with the corresponding estimate for a single SAP, which is also known to be bounded from below by $1/2$ [32]. Next, by assuming the validity of (8) at any β, we estimate the exponent ζ as a function of β (see Fig. 11). With the exception of a little variation in the proximity of the transition, it seems clear that ζ remains very close to the $\beta = 0$ estimate for all β values. Thus, the denaturation transition does not seem to affect the exponent of the power law dependence on N of the absolute value of the writhe. This is not surprising if one observes that for $\beta < \beta_c$ the two circular strands behave essentially as two independent SAP's, whereas for $\beta > \beta_c$ the two strands are tightly bound together forming a ribbon-like structure. Indeed the square root of N behavior of the absolute value of the writhe has been found also for the two boundaries of an orientable lattice ribbon model [28–30]. This confirms, also from the geometrical point of view, the good correspondence between the native regime of our model and the lattice ribbon model for double stranded molecules. The deviations of ζ from $1/2$ observed in the neighborhood of β_c are probably due to finite size effects. However, we can not exclude that a peculiar, distinct scaling regime prevails right at the transition. We know that there the statistics of denaturated loops is completely different from that at $\beta > \beta_c$ and this could imply a modification in the scaling behavior of $\langle|Wr|\rangle$. To establish whether a distinct scaling of $\langle|Wr|\rangle$ exists would be, however, very challenging numerically and beyond the scope of the present work.

5 Conclusions

In this paper we have studied the topological and geometrical entanglement of a lattice model for circular double stranded DNA undergoing a denaturation transition. We have shown that, in the limit of very long chains, the linking probability between the two strands is a function of β in the denatured phase, whereas it jumps very rapidly to values close to unity as soon as $\beta > \beta_c$, *i.e.* in the bound state. This feature is confirmed by the behavior of the average linking number in the two phases: it turns out that $\langle |Lk| \rangle$ is a small constant for $\beta < \beta_c$ and grows roughly as $\sqrt{N}$ in the low T phase. This suggests that our model in the native phase is, as far as the homological linking is concerned, similar to a ribbon model. This analogy is also confirmed by the behavior of the absolute value of the writhe as a function of β. In particular $\langle |Wr| \rangle$ roughly scales with N as $N^{0.51}$ for all β's and no supercoiling effects have been observed in this model of denaturation. This can be explained as follows: in our model the linking number is not fixed to a particular value and can fluctuate freely in the equilibrium statistics. Experimentally this would correspond, at least qualitatively, to the presence in the solution of the topoisomerases whose function is to change the linking number continuously. A different scenario can show up if instead the system is constrained to have a fixed linking number (no topoisomerases in solution). Indeed the fact that, for our model with unconstrained topology, the probability of being linked undergoes, right at denaturation, an abrupt (first order like) jump, suggests that the imposition of a constraint on the topology of the dsDNA molecule (by fixing the linking number between the two SAP's in our model) would affect rather sensibly some features of the transition, such as the melting temperature. There are indeed experimental indications that supercoiled structures characterized by a large (fixed) linking number, display a melting transition at higher temperatures than DNA molecules in the relaxed state [12].

References

1. K. Shishido, N. Komiyama, S. Ikawa, J. Mol. Biol. **185**, 215 (1987)
2. F.B. Dean, A. Stasiak, T. Koller, N.R. Cozzarelli, J. Biol. Chem. **260**, 4795 (1985)
3. C.D. Lima, J.C. Wang, A. Mondragon, Nature **367**, 138 (1994)
4. S.A. Wasserman, N.R. Cozzarelli, J. Biol. Chem. **266**, 20567 (1991)
5. J. Roca, J.C. Wang, Cell **77**, 609 (1994)
6. J.H. White, Am. J. Math. **91**, 693 (1969)
7. F.B. Fuller, Proc. Nat. Acad. Sci. USA **68**, 815 (1971)
8. N.R. Cozzarelli, *DNA Topology and Its Biological Effects*, edited by Cold Spring Harbor Laboratory Press (Cold Spring Harbor, NY, 1990)
9. A.V. Vologodskii, N.R. Cozzarelli Annu. Rev. Biophys. Biomol Struct. **23**, 609 (1994)
10. J. Vinograd, J. Lebowitz, R. Radloff, R. Watson, P. Laipis, Proc. Natl. Acad. Sci. USA **53**, 1104 (1965)
11. R.L. Burke, W. Bauer, Nucleic Acids Res. **5**, 4819 (1978)
12. A.V. Gagua, B.N. Belintev, Y.L. Lyubchenko, Nature **294**, 662 (1981)
13. P. Poland, H.A. Sheraga, J. Chem. Phys. **45**, 1456 (1966)
14. M.S. Causo, B. Coluzzi, P. Grassberger, Phys. Rev. E **62**, 3958 (2000)
15. Y. Kafri, D. Mukamel, L. Peliti, Phys. Rev. Lett. **85**, 4988 (2000)
16. E. Carlon, E. Orlandini, A.L. Stella, Phys. Rev. Lett. **88**, 198101 (2002)
17. N. Theodorakopoulos, T. Dauxois, M. Peyrard, Phys. Rev. Lett. **85**, 6 (2000)
18. D. Cule, T. Hwa, Phys. Rev. Lett. **79**, 2375 (1997)
19. J. Rudnick, R. Bruinsma, Phys. Rev. E **65**, 030902(R) (2002)
20. The model with strictly short range interactions has been used for a study of mechanical denaturation of DNA by E. Orlandini, S. Bhattacharjee, D. Marenduzzo, A. Maritan, F. Seno, J. Phys. A **34**, L751 (2001)
21. M.C. Tesi, E.J. Janse van Rensburg, E. Orlandini, S.G. Whittington, J. Stat. Phys. **82**, 155 (1996)
22. N. Madras, A. Orlitsky, L.A. Shepp, J. Stat. Phys. **58**, 159 (1990)
23. P.H. Verdier, W.H. Stockmayer, J. Chem. Phys. **36**, 227 (1961)
24. A.M. Ferrenberg, R.H. Swendsen, Phys. Rev. Lett. **61**, 2635 (1988); **63**, 1195 (1989)
25. W.R. Bauer, F.H. Crick, J.H. White, Sci. Am. **243**, 118 (1980)
26. D. Rolfsen, *Knots and Links* (Publish or Perish, Inc., Wilmington, 1976)
27. E. Orlandini, E.J. Janse van Rensburg, M.C. Tesi, S.G. Whittington, J. Phys. A **27**, 335 (1994)
28. E.J. Janse van Rensburg, E. Orlandini, D.W. Sumners, M.C. Tesi, S.G. Whittington, Phys. Rev. E **50**, R4279 (1994)
29. E.J. Janse van Rensburg, E. Orlandini, D.W. Sumners, M.C. Tesi, S.G. Whittington, J. Stat. Phys. **85**, 103 (1996)
30. E. Orlandini, E.J. Janse van Rensburg, S.G. Whittington, J. Stat. Phys. **82**, 1159 (1996)
31. R.C. Lacher, D.W. Sumners, *Data Structures and Algorithms for the computation of topological invariants of entanglements: link, twist and writhe,* in *Computer Simulations of Polymers*, edited by R.J. Roe (Prentice-Hall, 1991), p. 365
32. E.J. Janse van Rensburg, E. Orlandini, D.W. Sumners, M.C. Tesi, S.G. Whittington, J. Phys. A **26**, L981 (1993)